IGF 11 - XI Convegno Nazionale
Gruppo Italiano Frattura
Brescia, 4-6 luglio 1995

FRACTURE RESPONSE OF PARTICULATE ALUMINA-ZIRCONIA COMPOSITES

G. Nicoletto°, A. Tucci*, L. Esposito*

(°) Dip. di Ingegneria Industriale,
Università di Parma
Viale delle Scienze - 43100 Parma

(*) Centro Ceramico
Via Martelli, 26 - 40138 Bologna

Abstract

After an initial brief review of the peculiar features of the alumina/zirconia material system and the presentation of the main toughening mechanisms expected in a particulate composite, the fracture response of zirconia-based particulate composites is investigated with the indentation toughness and the SEPB methods. Crack morphology is investigated in the SEM to help identify the toughening mechanisms behind the material response.

1. Introduction

The resistance of brittle solids to the propagation of cracks can be strongly influenced by microstructure and by the use of various reinforcements which result in the activation of individual toughening mechanisms such as phase transformations, microcracking, grain bridging, crack deflection ecc, [1]. A toughening mechanism modifies the stress intensity at the crack tip K_{tip} from the far-field value K_{∞} which is controlled by the geometry, crack length and applied stresses and, therefore, increase the fracture toughness.

Zirconia-based ceramics are a typical example of materials whose toughness can be enhanced by microstructural design, [2]. In this paper we initially review the motivations and the potential benefits behind the development of particulate alumina/zirconia materials, then we outline the toughening mechanisms most likely found in a brittle particulate composite. We subsequently present the experimental procedures used to characterize the fracture response of various alumina/zirconia composites and discuss these results in the light of scanning electron microscopic observations of the crack-microstructure interaction.

2. Toughening mechanisms in the alumina/zirconia system

Zirconia has found great appeal at the time of the discovery of the now well-known tetragonal (high temperature) to monoclinic (low temperature) phase transformation, which is characterized by a large volume change (3-5%) and shear deformation (1-7%), [2]. This stress-assisted martensitic phase change takes place in the material surrounding the crack tip and has been exploited for improving the toughness of zirconia-based ceramics. The possibility of retaining the tetragonal phase at room temperature by addition of various stabilisers such as MgO, Y_2O_3 and CeO_2 has led to the development of a wide range of microstructures, from completely tetragonal zirconia polycrystals (TZP) to tetragonal precipitates in a cubic zirconia matrix (PSZ), [2].

The service temperature, however, significantly influences the toughness of these transformation materials. At higher temperatures the tetragonal phase is more stable (i.e. phase transformation energetically more difficult above 700°C for Yttria-TZP) and the fracture toughness decreases. Reinforcing components such as fibers and particulates are added to offset these problems. Alumina is probably the best reinforcement material for use in a TZP matrix because it increases the modulus of elasticity, prevents the developments of large grains in the zirconia cubic phase (often present in TZP ceramics), has high thermal stability and a low thermal mismatch with the TZP matrix. In addition, the alumina particles interact with a propagating crack activating toughening mechanisms.

An alternative particulate composite material making use of the martensitic transformation is obtained by the addition of zirconia dispersoids into in an alumina matrix, also known as zirconia-toughened alumina (ZTA). It is expected to have a higher toughness and strength with respect to pure alumina because toughening mechanisms such as martensitic transformation and stress-induced microcracking can be activated, [3].

The main toughening mechanisms expected in zirconia/alumina material systems are now briefly reviewed to help in understanding the results of the experimental portion of the study. Some mechanisms affect the process zone ahead of the crack tip, others operate in the wake of the propagating crack. In principle, material systems could present more than one toughening mechanism with a synergistic effect, [1].

2.1 Stress-induced transformation

In partially-stabilized zirconia the high stresses in the process zone ahead of the advancing crack tip interacts with and promote the martensitic phase transformation. Expansion of the transforming particles induces residual compressive stresses in the monoclinic zirconia matrix where the crack tip is advancing. An effective reduction of the crack tip stress results from superposition as schematically shown in Fig. 1a, [4].

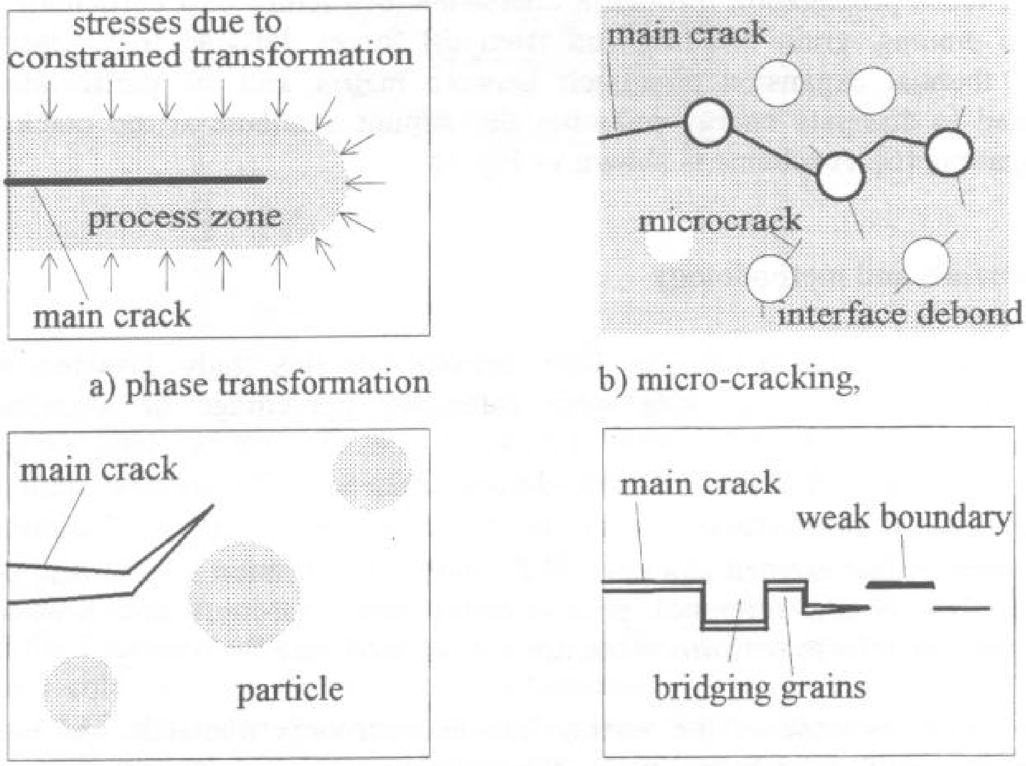

a) phase transformation b) micro-cracking,

c) crack deflection d) grain bridging

Fig. 1 Schemes of the main toughening mechanisms

2.2 Microcracking

Composite systems characterized by zirconia particles embedded in an alumina matrix undergo a volumetric expansion upon cooling below the tetragonal to monoclinic transformation temperature. The large volume change is sufficient to exceed the elastic and the fracture limits even in small grains. Therefore, micro-fractures may develop at the interphase and in the surrounding alumina, [3]. A propagating crack interacting with the particle dissipate energy by frictional sliding and by crack deflection according to the scheme of Fig. 1b. The toughening can be maximized by zirconia volume fraction control. Above certain levels the particles may interact reducing the global effect on the crack tip.

2.3 Crack deflection

Second phase particles located in the near tip field of a propagating crack perturb the front causing a reduction of the stress intensity. The reduction depends on the characteristics of the particles and on the nature of crack-particle interaction. Deflection toughening arises whenever interaction between the crack front and the particle produces a non planar crack subject to a stress intensity lower than that experienced by the straight crack, see Fig. 1c, [5].

2.4 Grain bridging

The crack tip stress intensity is affected also by the behavior of the crack surfaces in its wake. In the case of an ideally flat crack no surface interaction occurs. However, in the case of crack propagation through a coarse microstructure or a particulate composite, surface pinning, grain bridging and frictional forces deriving from elastic modulus and/or thermal expansion mismatch between matrix and the particulate phase are expected to dissipate energy reducing the amount available at the crack tip for the propagation, [6]. A scheme is shown in Fig. 1d.

3. Materials and methodology

The alumina/zirconia system has been examined in this study. Powders of 3% mol. Yttria-stabilized zirconia with with increasing percentage of alumina (TZ3YS, Z3Y20A, TZ3Y40A, TZ3Y60A, TZ3Y80A, i.e. 0%, 20%, 40% 60% and 80% alumina, respectively, from Tosoh, Japan) were used to prepare samples by slip casting. The microstructural morphologies were characterized by submicronic average grain sizes. A fine grained alumina (SM8, Baikowski, France, d = 2.3μm) powder was also used to obtain reference pure alumina data. Hardness and bending strength characterization were performed but are not reported here for brevity.

The fracture response of the various alumina/ zirconia materials has been initially investigated with the cost and time effective indentation fracture toughness technique, [7]. The method is widely used to estimate the fracture toughness of ceramic materials from length measurements of the cracks developing at the corners of the pyramidal shaped impression left on the material surface by a Vickers indentation. Depending on the crack system, the indenter geometry and the nature of the material, a variety of formulas have been proposed for fracture toughness estimation, [7]. As an example of the formula dependent variability of the indentation toughness, the estimates obtained by eleven formulas from the literature are presented for the TZ3YS material in Fig. 2. While the indentation load dependence for each formula is limited, the formula-dependent scatter is large: indentation toughness ranges from as low as 3.8 MPa $m^{1/2}$ to as high as 7 MPa $m^{1/2}$. The following equation for indentation toughness, K_{VI}, proposed in [8], was selected on the base of previous comparative studies, [7],

$$K_{VI} = 0.016\sqrt{\frac{E}{H}}\frac{P}{c^{3/2}}$$

where H is the hardness, P is the indentation load, E is the Young's modulus of elasticity and c is the semi crack length.

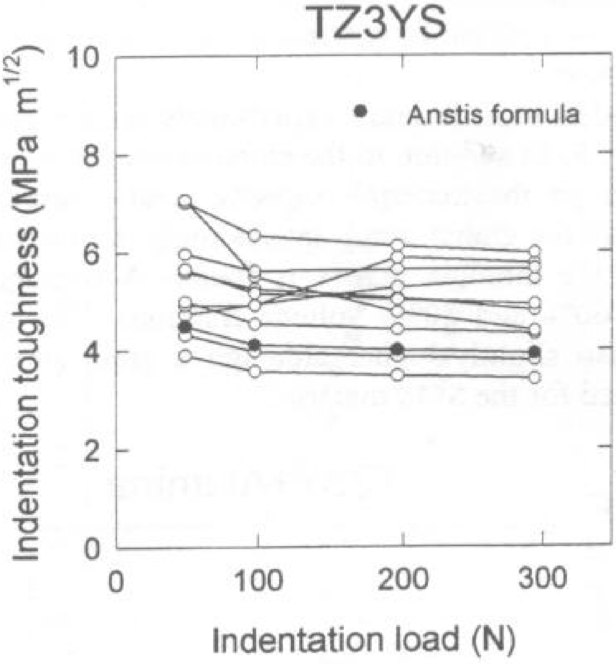

Fig. 2 Influence of indentation fracture formula

Due to the approximate nature of the indentation-based methods, a superior fracture toughness testing technique was used on selected material compositions, namely, the TZ3YS and the TZ3Y20A. Prismatic bars (3 x 4 x 50 mm^3) were respectively pressure slip cast and cold pressed, sintered and subsequently fine ground. The fracture technique used (SEPB technique) consisted of a two-phase procedure, [7,9]: i) the introduction of a natural edge precrack in a prismatic bar according to the bridge indentation technique, [9], and ii) the fracture test of the precracked bar under four-point bending loading. With respect to the indentation fracture technique, more material is required and relatively long cracks are tested. However, the precracked bar configuration permits the direct application of the standard calibration formulas for K_{IC} determination.

$$K_{IC} = Y\left(\frac{a}{W}\right)\frac{6M}{BW^2}\sqrt{\pi a}$$

where $Y(a/W)$ is the SENB calibration function, [9], M is the fracture bending load, B and W are width and thickness of the specimen cross-section and a is the precrack length. This method is steadily gaining acceptance for fracture toughness determination of ceramics and has been included in recent round-robin studies.

Indentation cracks, precracks and fracture surfaces were also examined in a scanning electron microscope (SEM) to investigate the crack-microstructure interaction in these material systems. An overview of the main observations are presented in the next section.

4. Results and discussion

4.1 Indentation toughness

A summary of the indentation fracture experiments on the alumina/zirconia material system is given in Fig. 3. In addition to the alumina content on toughness, the effect of two indentation loads on the material response is also displayed. Load effects are limited and do not alter the global trend. Interestingly, an increase in toughness for up to 40 % alumina in the zirconia matrix is found. A reduced toughness is instead measured at higher (60% and 80%) volume fractions. The reference pure alumina toughness value is also slightly higher although a grain size dependent toughening contribution is expected for the SM8 material.

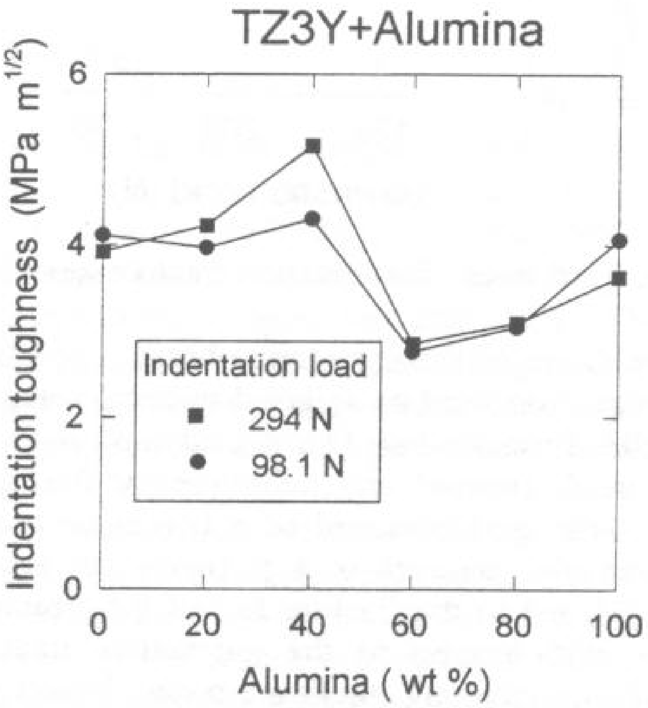

Fig. 3 Influence of alumina content on composite fracture by the indentation fracture technique

4.2 Fracture toughness

The previous observations are substantially supported by the fracture toughness measurements obtained with the SEPB method on two materials. The TZ3YS yields $K_{IC} = 3.4 \pm 0.28$ MPa m$^{1/2}$ while the 20% alumina-80% TZP composite (TZ3Y20AB) is characterized by $K_{IC} = 4.4 \pm 0.21$ MPa m$^{1/2}$. The absolute result for the TZP is not very high indicating that the phase transformation contribution on toughening is not marked. On the other hand, a significant increment (roughly 30%) in fracture toughness is found in the particulate composite with respect to the TZP material. This observation stresses the importance of the design of the microstructure for improved performance. The data are also introduced in the $ln(ln(1/(1-P))$ vs. $ln\ K_{IC}$ plot of Fig. 4 (P is the cumulative failure probability) where a two-parameter Weibull distribution yields a straight line. The data fit reasonably well the linear trend and a slope m=13.5

for the TZ3YS and $m = 25$ for the TZ3Y20AB is obtained by regression analysis. The high slope values indirectly support the reliability of the fracture testing technique.

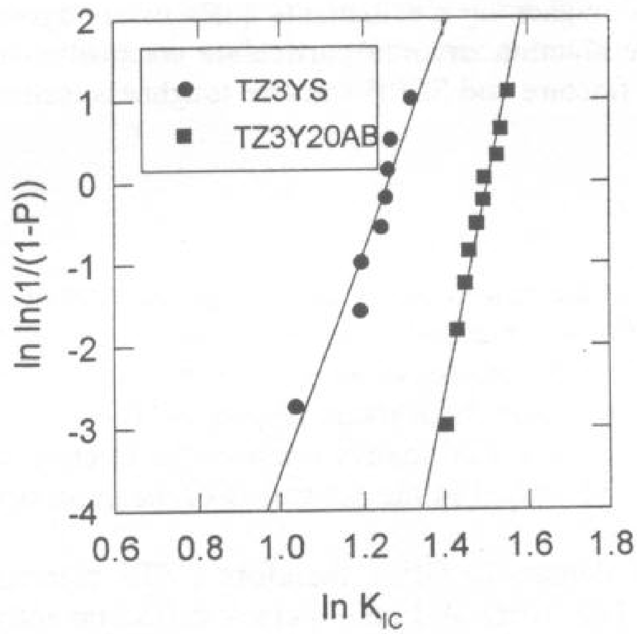

Fig. 4 Weibull plot of the SEPB fracture toughness

4.3 Fracture mechanisms

The main experimental findings obtained in the previous sections can be summarized as follows:

- a limited addition of alumina in a TZP matrix improves the fracture toughness with respect to the TZP material;
- a zirconia toughened alumina ZTA (high percentage of alumina and low percentage of TZP) seems to present a toughness comparable to the unreinforced materials (TZ3YS and SM8).

The identification of possible toughening mechanisms was the aim of a SEM investigation of the microstructure-crack interaction. Typical micrographs showing a crack in the TZP is in Fig. 5a, a crack in a TZP with 20% alumina (TZ3Y20AB) is in Fig 5b (the dark areas are the alumina particles) and a crack in a ZTA (alumina with 20% TZP) is in Fig. 5c. With respect to the four main toughening mechanisms previously outlined and schematically depicted in Fig. 1, inspection of Fig. 5 shows:

- in the TZ3YS no grain bridging and crack deflection are observed. The extent of the phase transformation is not determined directly, however, the fracture toughness value, being relatively low, suggests a limited effect;
- in the TZ3Y20A, no significant crack deflection is observed while grain bridging is present. Also, cracking occurs at particle/matrix interface. As far as the contribution of the phase transformation the remark of the previous point applies;

- in the TZ3Y80A, no grain bridging is observed while crack deflection is more significant than in the previous cases. Fracture occurs along alumina grain boundaries.

These observations on toughening mechanisms qualitatively agree with the role of the alumina content in the alumina/zirconia particulate composites which was identified during the indentation fracture and SEPB fracture toughness testing.

5 Conclusions

The fracture behavior of the alumina-zirconia composite system has been investigated using the indentation fracture method. Selected compositions were characterized also with the SEPB method. The microstructure-crack interaction has been investigated with the SEM to help explaining the fracture responses. The main conclusions are:

- 20% alumina particles in a TZP matrix improve the fracture toughness of roughly 30 %. The reason is identified in the activation of the grain bridging mechanism in the wake of the crack.
- a higher content of alumina (> 60%), therefore a ZTA material, results in a lower toughness than the TZP material. Limited crack deflection activated by the alumina grain boundary fracture is observed.

Acknowledgements

G.N. gratefully acknowledges partial support of this research by Ministero dell'Università e della Ricerca Scientifica e Tecnologica.

References

[1] A.G. Evans, "Perspective on the development of high-toughness ceramics", *J. Am. Ceram. Soc.*, 73, 2, (1990), pp.187-206

[2] R. Stevens, Zirconia and zirconia ceramics, Magnesium Elektron Ltd, 1986

[3] M. Ruhle, A.G. Evans, R.M. McMeeking, P.G. Charalambides, and J.W. Hutchinson, "Microcrack toughening in Alumina/Zirconia", *Acta Metall.*, 35, 11, 1987, pp.2701-10

[4] R.M. McMeeking, A.G. Evans, "Mechanics of transformation toughening in brittle materials", *J. Am. Ceram. Soc.*, 65, 5, (1982), pp.242-7

[5] K.T. Faber, A.G. Evans, "Crack deflection processes - I. Theory", *Acta Metall.*, 31, 4, (1983), pp. 565-576

[6] Y.W. Mai, B.R. Lawn, "Crack interface grain bridging as a fracture resistance mechanism in ceramics: II, Theoretical fracture mechanics model", *J. Am. Ceram. Soc.*, 70, 4, (1987), pp.289-94

[7] G. Nicoletto, L. Esposito, "Fracture toughness of ceramic materials by the precracked bend bar and the indentation methods", *Procs. XIX AIAS National Conference*, Pisa, (1991), pp.409-422

[8] G.R. Anstis, P. Chantikul, B.R. Lawn, D.B. Marshall, "A critical evaluation of indentation techniques for measuring fracture toughness: I, direct crack measurements", *J. Am. Ceram. Soc.*, 64, (1981), pp.533-8
[9] G. Nicoletto, M. Leccese, L. Esposito, "A method for the determination of mixed-mode fracture toughness of ceramic materials", *Ceram. Acta*, 5, 1-2, (1993), pp.59-71

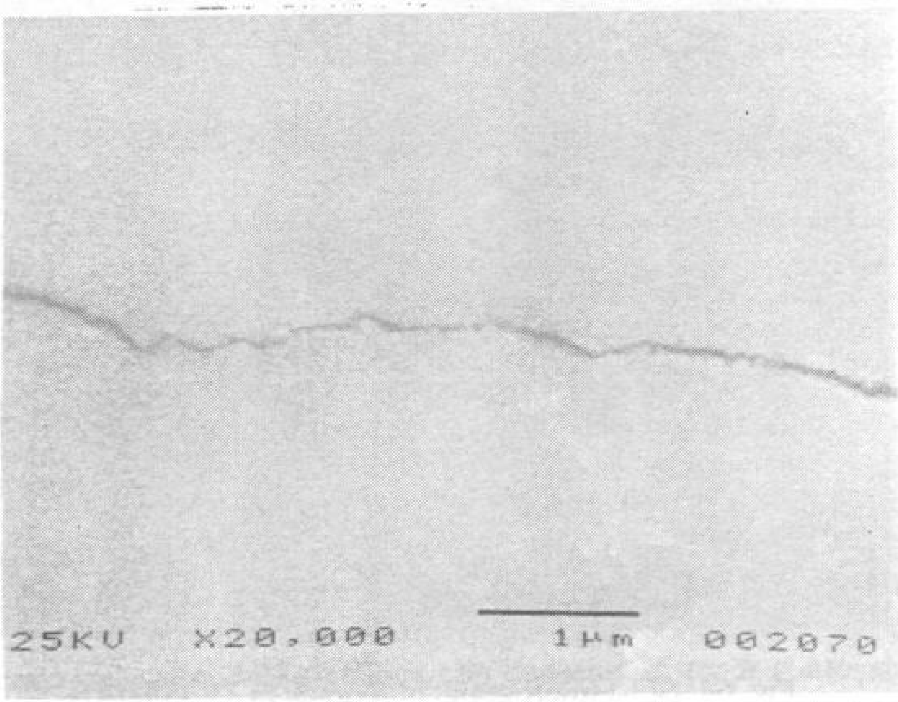

Fig. 5a SEM micrograph of a crack in TZ3YS

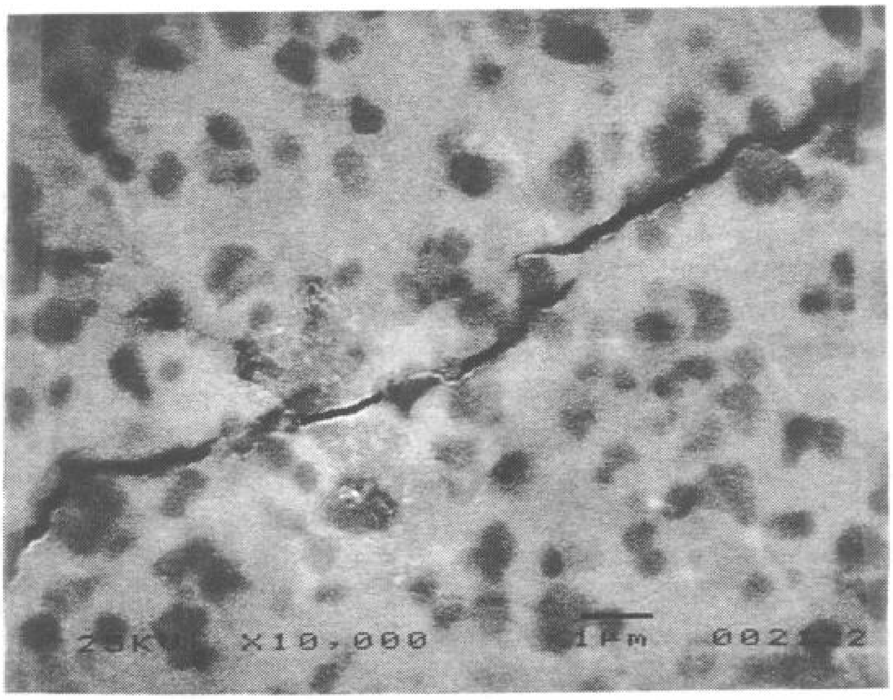

Fig. 5b SEM micrograph of a crack in TZ3Y20AB

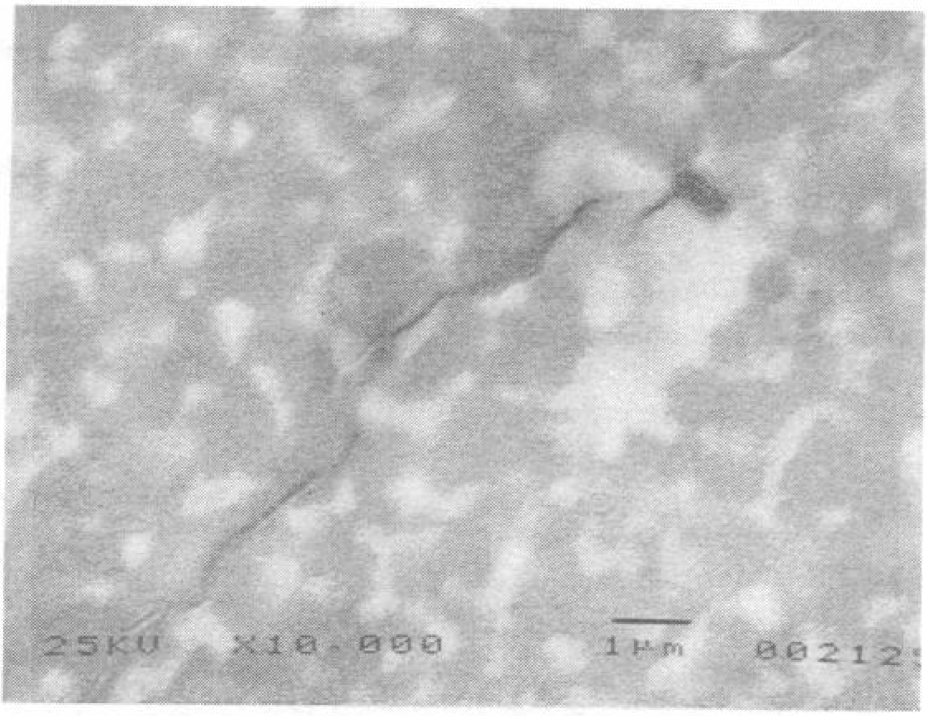

Fig. 5c SEM micrograph of a crack in TZ3Y80AB